

A Measurement of the Coulomb Dissociation of ${}^8\text{B}$ at 254 MeV/nucleon and the ${}^8\text{B}$ Solar Neutrino Flux

N. IWASA^{1,2}, F. BOUÉ^{1,3}, G. SURÓWKA^{1,4}, K. SÜMMERER¹, T. BAUMANN¹, B. BLANK³,
S. CZAJKOWSKI³, A. FÖRSTER⁵, M. GAI⁶, H. GEISSEL¹, E. GROSSE⁷, M. HELLSTRÖM¹,
P. KOCZON¹, B. KOHLMAYER⁸, R. KULESSA⁴, F. LAUE⁵, C. MARCHAND⁴,
T. MOTOBAYASHI⁹, H. OESCHLER⁵, A. OZAWA², M. S. PRAVIKOFF³, E. SCHWAB¹,
W. SCHWAB¹, P. SENGER¹, J. SPEER⁸, C. STURM⁵, A. SUROWIEC¹, T. TERANISHI²,
F. UHLIG⁵, A. WAGNER⁵, W. WALUS⁴, and C.A. BERTULANI¹⁰

¹ *Gesellschaft für Schwerionenforschung m.b.H. (GSI), D-64291 Darmstadt, Germany.*

² *RIKEN (Institute of Physical and Chemical Research), Wako, Saitama 351-0198, Japan.*

³ *Centre d'Etudes Nucléaires de Bordeaux-Gradignan, F-33175 Gradignan, France.*

⁴ *Jagellonian University, PL-30-059 Krakow, Poland.*

⁵ *Technical University of Darmstadt, D-64289 Darmstadt, Germany.*

⁶ *University of Connecticut, Storrs, CT 06269-3046, U.S.A.*

⁷ *Forschungszentrum Rossendorf, D-01314 Dresden, Germany.*

⁸ *Marburg University, D-35032 Marburg, Germany.*

⁹ *Rikkyo University, Toshima, Tokyo 171, Japan.*

¹⁰ *Instituto de Fisica, Universidade Federal do Rio de Janeiro, 21945-970 RJ, Brazil.*

Abstract

We have measured the Coulomb dissociation of ${}^8\text{B}$ into ${}^7\text{Be}$ and proton at 254 MeV/nucleon using a large-acceptance focusing spectrometer. The astrophysical S_{17} factor for the ${}^7\text{Be}(\text{p},\gamma){}^8\text{B}$ reaction at $E_{\text{c.m.}} = 0.25\text{--}2.78$ MeV is deduced yielding $S_{17}(0) = 20.6 \pm 1.2$ (exp.) ± 1.0 (theo.) eV-b. This result agrees with the presently adopted zero-energy S_{17} factor obtained in direct-reaction measurements and with the results of other Coulomb-dissociation studies performed at 46.5 and 51.2 MeV/nucleon.

PACs: 25.40.Lw, 25.60.-t, 25.70.De, 26.65.+t

The precise knowledge of the solar thermonuclear fusion of ${}^8\text{B}$ (from ${}^7\text{Be}$ plus proton) is crucial for estimating the ${}^8\text{B}$ solar neutrino flux and the predicted neutrino rates in terrestrial neutrino measurements. The relevant ${}^7\text{Be}(\text{p},\gamma){}^8\text{B}$ cross section $\sigma(E)$ is parameterized in terms of the astrophysical factor $S_{17}(E)$ which is defined by $S_{17}(E) = \sigma(E)E \exp[2\pi\eta(E)]$ where $\eta(E) = Z_1Z_2e^2/\hbar v$ is the Sommerfeld parameter. The flux of ${}^8\text{B}$ solar neutrinos is particularly important for the results of the Homestake, Super Kamiokande, and SNO experiments [1] which measure high-energy solar neutrinos mainly or solely from the ${}^8\text{B}$ decay.

Unfortunately, this cross section has not been known with sufficient accuracy for a long time, despite the fact that several comprehensive direct measurements were reported for the ${}^7\text{Be}(\text{p},\gamma){}^8\text{B}$ reaction [2–6]. The main difficulty in such experiments is the determination of the effective target thickness of the radioactive ${}^7\text{Be}$ target. This difficulty is reflected in the fact that the results of these measurements can be grouped into two distinct data sets which agree in their energy dependence but disagree in their absolute normalization by about 30%. In view of this discrepancy, experimental studies with different methods are highly desirable.

As an alternative approach one can measure the inverse process, the Coulomb dissociation (CD) of ${}^8\text{B}$ into ${}^7\text{Be}$ and proton [7]. The CD yields are enhanced because thicker targets can be used and a larger phase space is available for CD. This method uses stable targets and thus is free from the difficulty of determining the effective target thickness. On the other hand, direct (p,γ) and Coulomb dissociation measurements have different sensitivities to the multipole composition of the photon fields. The E2 amplitude is enhanced in CD due to the large flux of E2 virtual photons, whereas it can be neglected in the (p,γ) reaction.

Recently, Motobayashi *et al.* have performed a CD experiment at $E({}^8\text{B}) = 46.5$ MeV/nucleon, yielding values for S_{17} in the energy range 0.6–1.7 MeV [8]. The extracted (p,γ) cross section is consistent with the results from the lower group of direct-reaction data points [4–6]. Another measurement at 51.9 MeV/nucleon by the same group with improved accuracy led essentially to the same conclusion [9].

In this article, we report on an experiment of the CD of ${}^8\text{B}$ at a higher energy of

254 MeV/nucleon performed at the SIS facility at GSI, Darmstadt, Germany. The present incident energy has several advantages compared to those used in Refs. [8,9]: (i) due to the strong forward focusing of the reaction products the magnetic spectrometer KaoS [10] was used for a kinematically complete measurement with high detection efficiency over a wider range of the p - ^7Be relative energy; (ii) effects that obscure the dominant contribution of E1 multipolarity to the CD, such as E2 admixtures and higher-order contributions, are reduced [11,12]; (iii) the M1 resonance peak at $E_{\text{rel}} = 0.63$ MeV is excited stronger and therefore can be used to check the accuracy of the invariant-mass calculation.

A ^8B beam was produced by fragmentation of a 350 MeV/nucleon ^{12}C beam from the SIS synchrotron impinging on an 8.01 g/cm^2 beryllium target. The beam was isotopically separated in the fragment separator (FRS) [13] and transported to the standard target position of the spectrometer KaoS [10]. The average beam energy of ^8B at the center of the breakup target was 254.0 MeV/nucleon, a typical ^8B intensity was $10^4/\text{spill}$ with 7s extraction time. Beam particles were identified event by event with the TOF- ΔE method by using a plastic scintillator with a thickness of 5 mm placed 68 m upstream from the target and a large-area scintillator wall placed close to the focal plane of KaoS. About 20 % of the beam particles were ^7Be , which could however unambiguously be discriminated from breakup ^7Be particles by their time of flight.

An enriched ^{208}Pb target with a thickness of $199.7 (\pm 0.2) \text{ mg/cm}^2$ and with an effective area of $20 \times 22 \text{ mm}^2$ was placed at the standard target position of KaoS. The reaction products, ^7Be and proton, were analyzed by the spectrometer which has a large momentum acceptance of $p_{\text{max}}/p_{\text{min}} \approx 2$ and an angular acceptance of 140 and 280 mrad in horizontal and vertical directions, respectively. Two pairs of silicon micro-strip detectors, installed at about 14 and 31 cm downstream from the target, measured the x- and y-positions and hence the scattering angles of the reaction products in front of the KaoS magnets. Each strip detector had a thickness of $300 \mu\text{m}$, an active area of $56 \times 56 \text{ mm}^2$, and a strip pitch of 0.1 mm. The energy deposited on each strip was recorded using an analog-multiplexing technique. This configuration enabled us to measure opening angles of the reaction products

with a 1σ -accuracy of 4.8 mrad which is mainly caused by angular straggling in the relatively thick Pb target. By reconstructing the vertex at the target with an 1σ -accuracy of 0.3 mm, background events produced in the target frame or in the strip detectors could be largely eliminated. The remaining background events were found without the target under the same condition to be less than 0.5% of the true events.

Momenta of the reaction products were analyzed by trajectory reconstruction using position information from the micro-strip detectors and two two-dimensional multi-wire proportional chambers (MWPC) which detected the protons or the Be ions close to the focal plane of KaoS with a position resolution of about 1 mm.

A large-area ($180 \times 40 \text{ cm}^2$) scintillator wall [10] consisting of 30 plastic scintillator paddles with a thickness of 2 cm each was placed just behind the MWPC. It served as a trigger detector for the data acquisition system and as a stop detector for time-of-flight (TOF) measurements. To distinguish breakup events from non-interacting beam particles, the TOF wall was subdivided into two equal-size sections. The breakup events were characterized by coincident hits in the low-momentum (proton) and high-momentum (${}^7\text{Be}$ etc.) sections of the wall. The beam normalization was done by analyzing ${}^8\text{B}$ single hits on the high-momentum section (downscaled by a factor of 1000) under the condition (from the tracking information) that they originated from the active target area. From the measured angles and momenta of the breakup products the p- ${}^7\text{Be}$ relative energy and the scattering angle θ_8 of the center-of-mass of proton and ${}^7\text{Be}$ (i.e. the excited ${}^8\text{B}$) with respect to the incoming beam were reconstructed.

The p- ${}^7\text{Be}$ coincidence yield is shown in Fig. 1 (a) as a function of the p- ${}^7\text{Be}$ relative energy. It is obvious from the figure that, contrary to the direct measurements, the M1 resonance at $E_{\text{rel}} = 0.63 \text{ MeV}$ is not very pronounced. This is related to the energy resolution of our experiment (see below), and also to the relatively low sensitivity of CD to M1 transitions.

To evaluate the response of the detector system, Monte-Carlo simulations were performed using the code GEANT. The simulation took into account e.g. the finite size of the Si strip

and MWPC detectors as well as our inability to discriminate proton and ${}^7\text{Be}$ for very small opening angle where both particles hit the same strip. Events were generated with probabilities proportional to the CD cross section calculated with a semi-classical formula [14]. For the M1 resonance at $E_{\text{rel}} = 0.63$ MeV, the (p,γ) cross section calculated from the total and gamma widths measured by Filippone *et al.* [5] was used. The non-resonant contribution was obtained by normalizing the E1 (p,γ) cross section calculated by Bertulani [15] with a scale factor of 1.20.

Further corrections in the simulation are due to the feeding of the excited state at 429 keV in ${}^7\text{Be}$. We used the result by Kikuchi *et al.* [16] who measured the γ -decay in coincidence with the CD of ${}^8\text{B}$.

The histograms in Fig. 1(a) show the simulated E1+M1 yields (solid) and E1 yields (dashed). As seen in this figure, the shape and magnitude of the experimental energy dependence are well reproduced. This indicates that the CD yield is well described by a combination of the M1 resonance and the pure E1 continuum. In the lower part of Fig. 1 we show that the total efficiency calculated by the GEANT simulation is high over the entire E_{rel} range covered in our study. From the Monte Carlo simulation we also estimate our relative-energy resolution to be e.g. $\sigma(E_{\text{rel}}) = 0.11$ and 0.22 MeV at $E_{\text{rel}} = 0.6$ and 1.8 MeV, respectively.

In order to estimate upper limits for a possible E2 contribution to our yields, we have analyzed the θ_8 distributions. Since we did not measure the incident angle of ${}^8\text{B}$ at the target, the experimental angular distributions represent the θ_8 distributions folded with the angular spread of the incident beam. In Fig. 2, we plot the experimental yield against the scattering angle θ_8 for three relative-energy bins indicated in the figure; the contribution from the measured beam spread is shown in Fig. 2 (d). The full histograms represent the results of a Monte-Carlo simulation for E1 excitation using the theory of Bertulani [15], normalized to the experimental yield. The M1 transition also contributes to the 0.5–0.7 MeV bin with the same angular dependence. The simulated E2 angular distributions are also shown by the dashed histogram. The angular resolution was estimated to be 0.35 degrees (1σ), smaller

than the observed widths. As seen in the figure the experimental distributions are well reproduced by the simulation using E1 and M1 multipolarities, and no room is left to add an additional E2 component. The corresponding 3σ upper limits for the E2/E1 transition amplitude ratio are calculated from our model as $S_{\text{E}2}/S_{\text{E}1} = 0.06 \times 10^{-4}$, 0.3×10^{-4} and 0.6×10^{-4} for $E_{\text{rel}} = 0.3 - 0.5$, $0.5 - 0.7$, and $1.0 - 1.2$ MeV, respectively.

Recently, Esbensen and Bertsch have pointed out that interference between E1 and E2 components could play an important role in CD of ^8B and should manifest itself in an asymmetry of the longitudinal-momentum distribution of ^7Be [17]. Analyzing measured ^7Be momentum spectra in term of this model, Davids *et al.* [18] have deduced $S_{\text{E}2}/S_{\text{E}1} = 6.7_{-1.9}^{+2.8} \times 10^{-4}$ at 0.63 MeV which is much higher than our upper limits above. One should keep in mind, however, that such a strong E2 component need not necessarily affect the extraction of S_{17} : the dynamical calculation of Esbensen and Bertsch [17] at 45.6 \AA MeV shows that its effect can be much smaller than what is obtained by simply adding E1 and E2 components. Further experimental and theoretical studies are clearly desirable to clarify the magnitude of the E2 component in CD.

From the data and the simulation presented in Fig. 1 (a) we can deduce the astrophysical S_{17} factors for E1 multipolarity by scaling the theoretical S_{17} factors by the ratio of observed and simulated counts. The resulting S_{17} distribution is plotted in Fig. 3 as a function of the p- ^7Be relative energy, together with existing (p, γ) [4–6] and CD [9] results. The (p, γ) results were scaled to a peak cross section of the $^7\text{Li}(\text{d}, \text{p})^8\text{Li}$ reaction of 147 ± 11 mb [19]. The binning of our data was chosen to be approximately equal to the FWHM of the E_{rel} resolution. The errors shown in Fig. 3 result from summing in quadrature statistical errors and those resulting from uncertainties in the momentum calibration, in the angular cutoff of pure Coulomb processes, and in the feeding of the excited state in ^7Be . Since we are mostly interested in the E1 component, the simulated M1 component of the $E_{\text{rel}} = 0.63$ MeV resonance was subtracted from the data. At low E_{rel} , our results agree well with the lower group of the (p, γ) results [4–6] and the CD result of Kikuchi *et al.* [9]. We observe some discrepancies at higher E_{rel} , however, as shown in Fig. 3. While we cannot explain

the discrepancy with the RIKEN data [16], since all of the assumptions underlying their and our analysis are identical, the discrepancy to the direct measurements may be due to our neglect of an E2 component which, in a proper theoretical treatment, might affect the high- E_{rel} data points while leaving the low E_{rel} data virtually unchanged (see right-hand panel of Fig.11 in Ref. [17]).

Several theoretical models for ${}^8\text{B}$ have been proposed to predict the shape and magnitude of the S_{17} energy dependence, such as one-body potential models (see e.g. [11,15] for recent calculations) or more complex many-body (cluster) models (e.g. [20–23]). Our data in Fig. 3 follow very closely the results obtained by Bertulani [15] over the entire range of energies as indicated by the solid curve which was normalized to our data points using a scaling factor of 1.20. The shape of the distribution predicted by the cluster model calculation [20], which was favoured by the recent (p,γ) experiment of Hammache *et al.* [6], does not agree equally well with our results at the higher energies (dashed line in Fig. 3).

To obtain the zero-energy astrophysical S_{17} factor, we follow Jennings *et al.* [24] in fitting the theoretical energy dependence only to data points below $E_{\text{rel}} \approx 0.45$ MeV (see insert in Fig. 3) since this region should be largely free from uncertainties concerning nuclear excitations. From our two low E_{rel} data points we extracted $S_{17}(0) = 20.6 \pm 1.2 \pm 1.0$ eV-b where the first contribution results from fitting the data points of Fig. 3 and the second one is related to the uncertainty in extrapolating to zero E_{rel} . This result is compatible with the value of $S_{17}(0) = 19.0 \pm 1.0 \pm 0.2$ eV-b obtained by Jennings *et al.* [24] when fitting the combined data points of Refs. [5,6], and also with the adopted value of $S_{17}(0) = 19_{-2}^{+4}$ eV-b from Ref. [19]. We note, however, that the question of possible backscattering losses of recoiling nuclei in direct (p,γ) and (d,p) reactions [25,26] is not yet solved.

We conclude that we have demonstrated that high-energy Coulomb dissociation is very useful for determining the astrophysical S -factor of the ${}^7\text{Be}(\text{p},\gamma){}^8\text{B}$ reaction at low energies. We have used an analytical formula from the literature [24] to extrapolate our two low-energy S -factors to $S_{17}(0)$ and obtain a value that is consistent with the most recent compilation [19]. This supports essentially the standard-model prediction for the high-energy solar neutrino

flux [1].

We are grateful for the technical support by K.H. Behr, A. Brünle, and K. Burkard of the FRS staff. We thank N. Kurz for help with the data acquisition and J. Friese, R. Gernhäuser, E. Badura, and J. Hoffmann for their support in designing and realizing the Si micro-strip detector readout. Constant support and interesting discussions concerning the theoretical aspects were contributed by S. Typel, G. Baur, B.J. Jennings and H. Oberhummer. We thank P. Descouvemont and D. Baye for providing their numerical results.

REFERENCES

- [1] J.N. Bahcall *et al.*, Phys. Lett. B **433**, 1 (1998).
- [2] P.D. Parker *et al.*, Astrophys. J. **153**, L85 (1968).
- [3] R.W. Kavanagh *et al.*, Bull. Am. Phys. Soc. **14**, 1209 (1969).
- [4] F.J. Vaughn *et al.*, Phys. Rev. C **2**, 1657 (1970).
- [5] B. W. Filippone *et al.*, Phys. Rev. C **28**, 2222 (1983).
- [6] F. Hammache *et al.*, Phys. Rev. Lett. **80**, 928 (1998).
- [7] G. Baur and H. Rebel, Annu. Rev. Nucl. Part. Sci. **46**, 321 (1996).
- [8] T. Motobayashi *et al.*, Phys. Rev. Lett. **70**, 2680 (1994); N. Iwasa *et al.*, J. Phys. Soc. Japan **65**, 1256 (1996).
- [9] T. Kikuchi *et al.*, European Phys. J. A **3**, 213 (1998).
- [10] P. Senger *et al.*, Nucl. Instr. Meth. A **327**, 393 (1993).
- [11] S. Typel and G. Baur, Phys. Rev. C **50**, 2104 (1994); S. Typel *et al.*, Nucl. Phys. A **613**, 147 (1997).
- [12] C.A. Bertulani, Phys. Rev. C **49**, 2688 (1994).
- [13] H. Geissel *et al.*, Nucl. Instr. Meth. B **70**, 286 (1992).
- [14] C.A. Bertulani and G. Baur, Phys. Rep. **163** (1988) 300.
- [15] C.A. Bertulani, Z. Phys. A **356**, 293 (1996).
- [16] T. Kikuchi *et al.*, Phys. Lett. B **391**, 261 (1997), and priv. comm.
- [17] H. Esbensen and G.F. Bertsch, Nucl. Phys. A **600**, 37 (1997).
- [18] B. Davids *et al.*, Phys. Rev. Lett. **81**, 2209 (1998).

- [19] E.G. Adelberger *et al.*, Rev. Mod. Phys. **70**, 1265 (1998).
- [20] P. Descouvemont and D. Baye, Nucl. Phys. A **567**, 341 (1994).
- [21] C.W. Johnson *et al.*, Astrophys. J. **392**, 320 (1992).
- [22] A. Csótó *et al.*, Phys. Rev. C **52**, 1130 (1995).
- [23] L.V. Grigorenko *et al.*, Phys. Rev. C **57**, R2099 (1998).
- [24] B.K. Jennings *et al.*, Phys. Rev. C **58** (1998) 3711.
- [25] L. Weissman *et al.*, Nucl. Phys. A **630**, 678 (1998).
- [26] F. Strieder *et al.*, Eur. Phys. J. A **3**, 1 (1998).

FIGURES

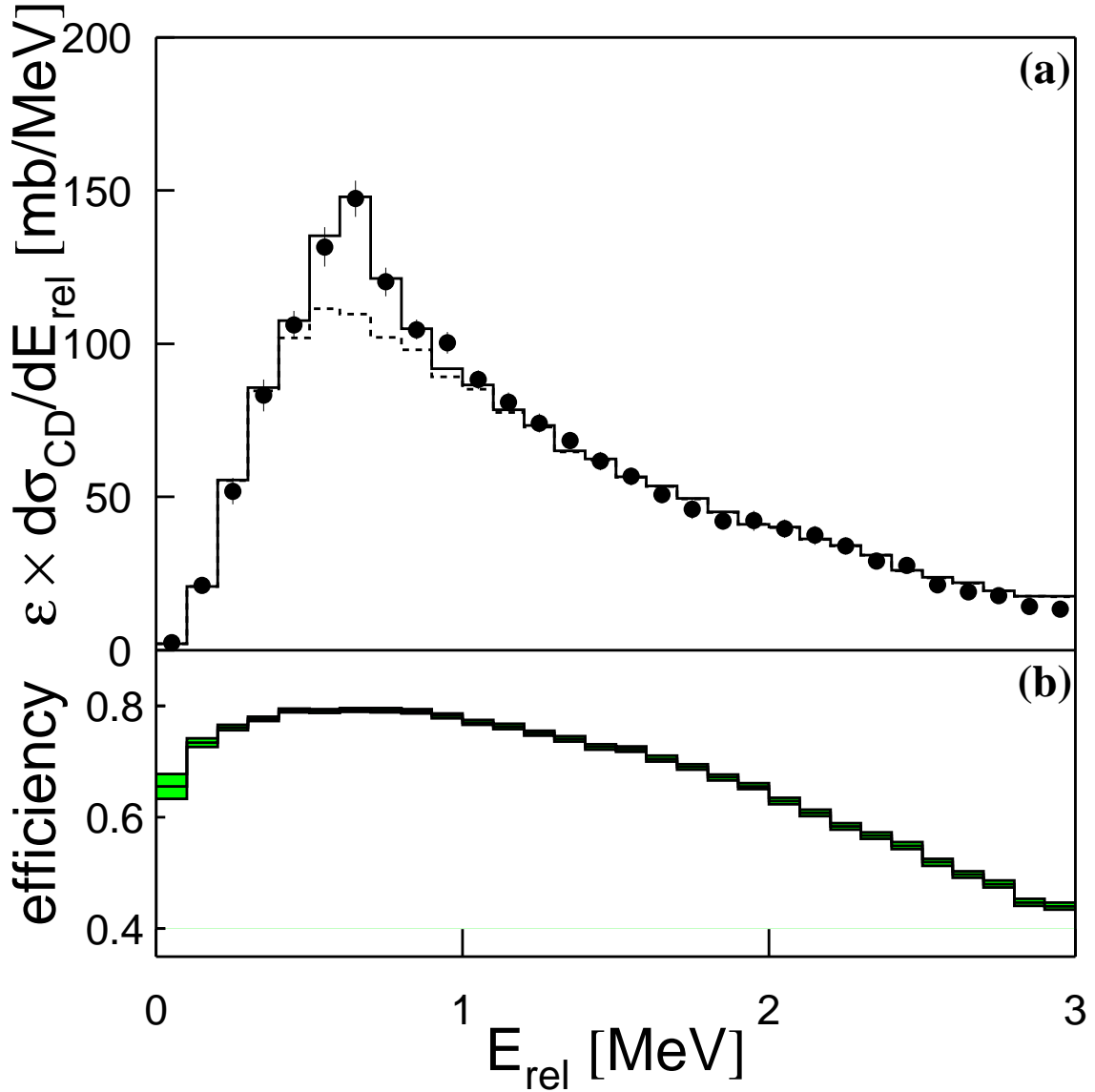


FIG. 1. (a) Yields of breakup events (cross section \times efficiency) plotted as a function of relative energy. The solid and dashed histograms denote simulated E1+M1 and E1 yields, respectively. (b) p-Be coincidence efficiency calculated by Monte Carlo simulations.

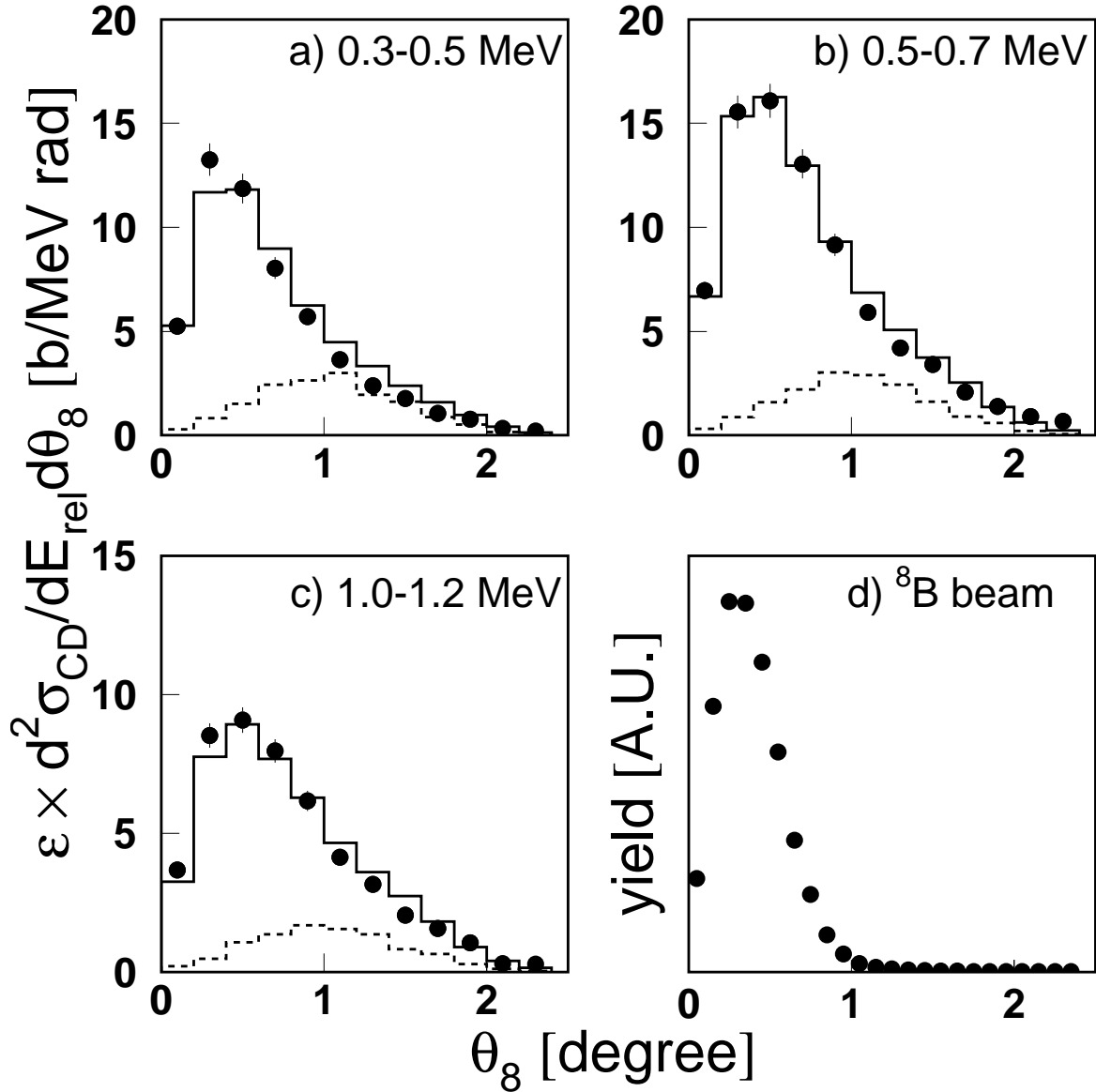


FIG. 2. (a,b,c)Yields of breakup events plotted against θ_8 , the scattering angle of the excited ${}^8\text{B}$, for three relative energy bins. The full histograms show the results of a simulation taking into account the measured angular spread of the incident ${}^8\text{B}$ beam (shown in d) and assuming E1+M1 multipolarity. The dashed histograms show the simulated results for E2 contribution according to the calculations of Bertulani [15].

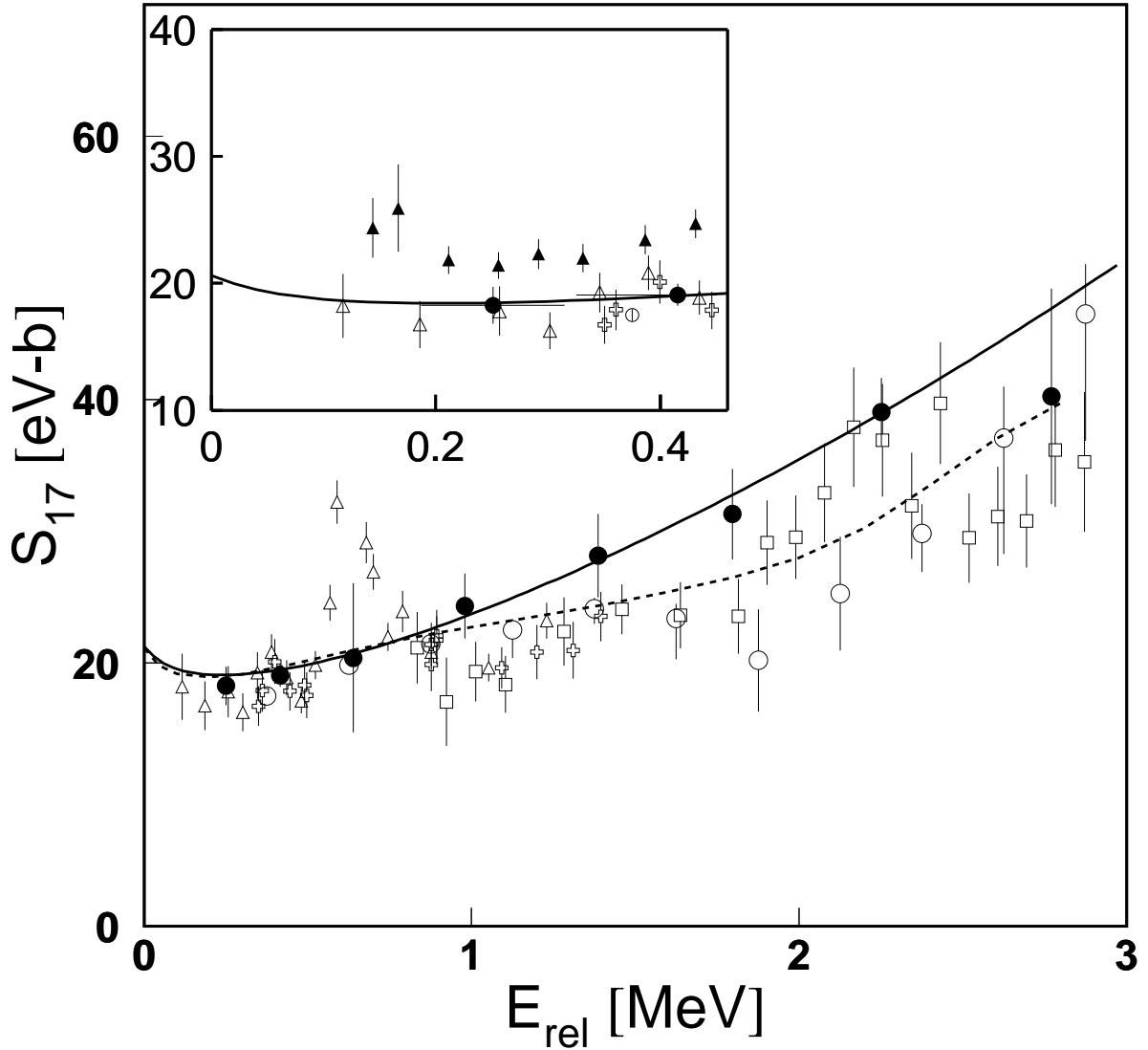


FIG. 3. The astrophysical S_{17} factors deduced from the present experiment plotted as a function of the $p\text{-}{}^7\text{Be}$ relative energy (closed circles), in comparison with results from direct and other Coulomb-dissociation experiments (closed triangles from [3], open boxes from [4], open triangles from [5], open crosses from [6], and open circles from [9]). The solid curve shows the prediction of Bertulani [15] fitted to our data, while the dashed curve shows a fit of the theoretical curve of Descouvemont *et al.* [20] to the combined datasets of Refs. [4–6]. The insert shows the low-energy part of the figure, where we have fitted the energy dependence of Jennings *et al.* [24] to our data.